Regular Article

# The electronic and optical properties of InGaN-based solar cells alloys: First-principles investigations via mBJLDA approach

A. Laref<sup>1,a</sup>, A. Altujar<sup>1</sup>, and S.J. Luo<sup>2</sup>

Department of Physics and Astronomy, College of Science, King Saud University, 11451 Riyadh, King. Saudi Arabia

Received 14 May 2013 / Received in final form 9 September 2013 Published online 18 November 2013 – © EDP Sciences, Società Italiana di Fisica, Springer-Verlag 2013

**Abstract.** First-principles calculations of the electronic and optical properties of the bulk  $In_xGa_{1-x}N$  alloys are simulated within the framework of full-potential linearized augmented plane-wave (FP-LAPW) method. To this end, a sufficiently adequate approach, namely modified Becke-Johnson (mBJLDA) exchange correlation potential is employed for calculating the energy band gap and optical absorption of InGaN-based solar cells systems. The quantities such as the energy gap, density of states, imaginary part of dielectric function, refractive index and absorption coefficient are determined for the bulk  $In_xGa_{1-x}N$  alloys, in the composition range from x=0 to x=1. It is found that the indium composition robustly controls the variation of band gap. From the examination of the density of states and optical absorption of  $In_xGa_{1-x}N$  ternary alloys, the energy gaps are significantly reduced for largest In concentration. The computed band gaps vary nonlinearly with the composition x. It is also surmised that the significant variation in the band gaps elaborated via the experimental crystalline growth process, is originated by altering the In composition. Interestingly, it is worthwhile to perform InGaN solar cells alloys with improved efficiencies, because of their entire energy gap variation from 0.7 to 3.3 eV.

# 1 Introduction

Over the recent years, the group-III nitride-based semiconductors have proved their potential application in the fabrication of optoelectronic devices because of their functionalities alteration from the ultraviolet to near-infrared. Among them, GaN, AlN, InN compounds and their corresponding alloys have been discerned to be excellent candidates for laser diodes and short-wavelength light emitting diodes [1–22]. These categories of wide band gap semiconductors have been revealed to be promising candidates for the absorber layers in solar cells, since their absorption edge can be altered to optimize the cell efficiency. Moreover, they exhibit high mechanical and thermal stabilities with respect to other III-V semiconductors. Their impressive characteristics made them particularly pertinent for the high-power and high-temperature operations. Also, III nitride-based semiconductors are appealing for multi-junction photovoltaic devices [14–22]. Importantly, In-incorporating nitride alloys are specifically suitable in several technological applications because of the particular role of indium. The increase of In into III-nitride semiconductors in low quantities, drives to an improvement of light emission intensity in laser diodes (LDs) and light emitting diodes (LEDs) [9–12]. Furthermore,  $In_xGa_{1-x}N$ -based solar cells and detectors can operate

in the short-wavelength interval and they have also been built up in various laboratories [1–12]. The recent success on nitride semiconductor devices is substantially related to the typical GaN compound and its corresponding alloys (InGaN, InAlN, and AlGaN). These materials can constitute ternary alloys with continuous wide range of direct band gaps. Even though the wurtzite structure is suitable for growing most III-nitride semiconductors, the zinc-blende structure still possesses specific advantage over the wurtzite crystal. For instance, the zinc-blende structure is revealed to have a lower threshold current density and a wider optical gain. This can be attributed to its small effective mass, and its mirror facets analogous to the substrates, like GaAs [23]. Then, the InGaN semiconductor alloys yield a typical factor for tailoring the magnitude of the forbidden gap and other related components, such as optimizing and broadening the application of semiconductor devices.

Several III-nitrides semiconductor properties possess the most favorable features because of their diverse technological applications. Recently,  $In_xGa_{1-x}N$  ternary alloys are emerged as new solar cell materials. This is due to the modulation of the energy band gaps (variation from 0.7 eV for  $\beta$ -InN and 3.3 eV for  $\beta$ -GaN to 4.9 eV for  $\beta$ -AlN [4–12], comprising practically the full solar spectrum) and superior photovoltaic features (direct energy gap in the whole alloy variation, high drift velocity,

<sup>&</sup>lt;sup>2</sup> School of Science, Hubei University of Automotive Technology, Shiyan City, Hubei, P.R. China

a e-mail: amel\_la06@yahoo.fr

radiation resistance, carrier mobility, and strong optical absorption of  $\sim 10^5$  cm<sup>-1</sup> nearby the band edge) [18,19]. Even though InGaN based solar cells provide tremendous potential for space and terrestrial photovoltaic applications, not many information on InGaN based solar cells alloys have been reported. In addition, many statements on InGaN solar cells claimed that the In composition inferior than 15% and band gaps near 3 eV, or wider, can consequently carry reduced quantum efficiency at wavelengths more than 420 nm [18,19]. It has been reported theoretically that the fulfillment of active materials can acquire solar cells with a solar energy conversion efficiency higher than 50% for InGaN alloys, if the In content is close to 40% [20]. Furthermore, for the greatest solar energy conversion efficiency, III-nitride multi-junction solar cells possessing a nearly perfect band gaps, should involve InGaN layers with higher In concentration or narrower energy band gaps.

In this work, we focus on the cubic phase of III-nitride semiconductors, namely GaN and InN and their ternary alloys because of their technological importance in the cubic nitride based devices. The crystalline growth of InGaN alloys was successfully performed particularly for the largest compositions of In in the ternary film (>30%). Accordingly, for films with various In compositions, the measured optical absorption constant exhibits a noticeable behavior in Ga<sub>0.63</sub>In<sub>0.37</sub>N which is less sharper than that of GaN and the InGaN films with low indium content [13]. The electronic structures and optical response spectra are usually required in optoelectronics research. Albeit the electronic and optical properties have been exclusively explored for GaN compound, there is still a need for the theoretical and experimental comprehension of  $In_xGa_{1-x}N$  alloys. This is due to the perplexity in designing InGaN samples with specific conditions of measurements [5–22]. Several recent studies have pointed out the outstanding synthesis of highcharacteristic  $In_xGa_{1-x}N$  alloys and  $In_xGa_{1-x}N$ -based nanostructures, like the superior-quality  $In_xGa_{1-x}N$  films,  $In_xGa_{1-x}N/GaN$  multiple quantum well solar cells and  $In_xGa_{1-x}N$  nanowires [24–34].

Certainly, theoretical researches based on the common first-principles schemes, have demonstrated an extensive benefit for the exploration of complicated materials. The adequate first principles calculations [35–40] are prosperous in predicting or corroborating the ground state properties for different systems. Therefore, some traditional exchange-correlation functional employed in density functional theory (DFT), such as the local density approximation (LDA) or generalized gradient approximation (GGA), are well recognized to underestimate the band-gap in various semiconductors and insulators. The critical issue for handling the narrow band gap semiconductors is related to the negative band gaps and hence inaccurate optical properties would be established. In this extreme situation for InN, the predicted band gap is rather negative, driving to a metal instead of a semiconductor [34,35]. Thus, the major deficiency for LDA or GGA is due to the lacking of the discontinuity for the exchange-correlation potential [39].

For instance, the computed band gaps of several semiconductors (e.g. GaN) are roughly underestimated against the experimental results [34,35]. This dilemma can be elucidated by utilizing various recently developed functionals for the exchange and correlation potential. Consequently, various theoretical schemes have been developed to ameliorate the band gap of diverse systems and corroborate well the experimental data. Several approaches and functionals have been developed so far to overcome the difficulties related to the optimized effective potential (OEP), many-body perturbation theory (MBPT), GW method and hybrid functionals [41–47] which take into account the energies of quasiparticles. These methods provide good flexibility, although they can operate beyond the DFT. It is well recognized that the GW scheme describes the energy gap results in very good accordance with respect to the experimental determinations [9–19,34], where it is computationally consuming for complex systems. However, the LDA + U approach is merely employed to the correlated and localized 3d and 4f electrons in transition and rare-earth oxides systems [48]. Fortunately, with low computational cost, the recently developed mBJLDA approach [49] is applicable to compute with sufficient accuracy the energy band gaps of several semiconductors with respect to the highly time consuming methods such as the GW and hybrid functionals.

On the other hand, the description of the electronic structure of different systems such as semiconductors, insulators, strongly correlated 3d transition-metal oxides, as well as the half-metallic compounds is fairly good by using the mBJLDA [49–55]. It is acclaimed to utilize the LDA or GGA based functional for calculating the structural properties. However, the mBJLDA potential is merely applied for computing the electronic properties [49–51]. With this technique, the predicted band gap values are highly ameliorated over the traditional LDA and GGA and are in good agreement with the experimental findings [34]. Diverse theoretical studies on III-V semiconductors evidently exhibit that the MBJ exchange potential in addition to the correlation part of LDA can treat the band gaps quite satisfactorily and the relative locations of some specific bands, e.g. band gap crossovers [49–51]. Most of previous experimental [9–19] and theoretical [34,35] researches have explored the band gap as a function of In content for wurtzite parent AlN, GaN, InN compounds and their corresponding alloys. Lately, improved band gaps of wurtzite AlGaN, InGaN and AlInN alloys have been computed within the LDA-1/2 approximation by Pelá et al. [56]. Other techniques have been also reported which are based on the hybrid functionals. As a consequence, they permit reasonably adequate energy gap calculations and can be utilized for III-nitride compounds. For instance, by taking into account the hybrid exchange-correlation functional of Heyd, Scuseria and Ernezerhof (HSE) [57,58], the recent work pointed out by Moses and de Walle [59] provides a satisfactorily accurate description of the energy band gap of wurtzite InGaN alloys.

Due to their technological consideration, a precise prediction for the optical properties of III-nitride alloys is significantly attractive. To the best of our knowledge, first-principles investigations based on DFT for investigating the optical properties of InGaN alloys are barely pointed out. The purpose of this study is to explore theoretically the electronic and optical characteristics of the parent InN and GaN compounds and their ternary alloys by utilizing FP-LAPW scheme [60]. For a fairly good description of the energy band gaps of our considered systems, the mBJLDA has been employed for handling the exchange and correlation term. This paper is organized as follows: in Section 2, we outline briefly the computational method which corresponds to the current calculations. Section 3 treats our results for the electronic and optical properties of bulk InGaN alloys and more precisely the density of states, band gap bowing, dielectric function, optical absorption coefficient and refractive index are discussed. So, we focus our analysis on the compositional effect of the electronic and optical properties of  $In_xGa_{1-x}N$  alloys. Our theoretical findings based on mBJLDA reproduce quite well the electronic and optical features in comparison with the other theoretical works and available experimental data. Our results demonstrate that the In-incorporation in GaN would dramatically ameliorate the optical behavior of  $In_xGa_{1-x}N$  alloys. Indeed this may lead to the significant improvement of the efficiency of the state-of-the-art InGaN-based solar cells. The essential points of the conclusion are drawn in Section 4.

# 2 Computational method

In this current study, we explore the effect of In concentration on the electronic and optical properties of  $In_xGa_{1-x}N$ alloys by adopting FPLAW method, as embodied in the Wien2K code [60]. In our simulation, we set appropriate parameters for providing enough precise results concerning the physical properties of these systems. In the full potential scheme, the expansion of the potential and charge density are described in terms of spherical harmonics interior the muffin-tin spheres, while the plane waves basis set are located in the interstitial region. The wave function expanded inward the atomic spheres is set with the l value limit up to  $l_{\text{max}} = 10$ . The muffin-tin radii are adopted to be 2.3 a.u, 2.2 a.u and 1.45 a.u for In, Ga and N, respectively, whereas the leakage of charge will not appear from the core and then the total energy is converged. Here, the convergence of the basis set is controlled by a cutoff parameter  $R_{\rm mt}K_{\rm max}=8$ , although the Fourier expansion of the charge density is selected up to  $G_{\rm max}=12$  Ryd.  $R_{\rm mt}$  is the smallest muffin tin radius of the atomic spheres in the unit cell. All the integrations in the Brillouin zone (BZ) are based on tetrahedron scheme by utilizing a sampling grid of 8000 k-points. In this case, a good convergence was obtained after performing different tests of calculations with different grids of k-points up to 8000 k-points. For the total energy calculations, we utilize the Perdew-Wang [40] functional for exchange and correlation in LDA. Furthermore the mBJLDA was employed for the electronic and optical calculations. For binary and alloy compounds

(GaN, InN and InGaN), we optimized the structural geometries by minimizing the total energy with respect to the cell parameters where the Perdew-Wang [40] functional for exchange and correlation in LDA is used [40]. For the fully relaxed InGaN alloys, we modeled ordered structures with cubic supercell of eight atoms/unit cell (supercell techniques), containing four nitrogen atoms and four Ga atoms, e.g. for GaN. In this case, we can select all possible compositions of In variation between 0\%, 25\%, 50%, 75%, and 100%. By this way we can set all possible configurations with the mixture between Ga and In atoms in order to form  $In_xGa_{1-x}N$  alloys. As it has been stated previously that InGaN solar cells with In composition less than 15% and band gaps close to 3 eV, or greater, these systems may hold a reduction of quantum efficiency for wavelengths more than 420 nm [18,19]. For this purpose, we did not investigate III-nitride diluted alloys with low In concentration. Since from the experimental realizations, the active materials can achieve solar cells with a solar energy conversion efficiency higher than 50% for InGaN alloys, if the incorporation of InN fractions is between 30% and 40% [20]. However, by taking eight atoms in the cubic supercell with 25%, 50% and 75% variation of In content, we can cover the compositions range that were realized experimentally [20]. Then, this can make these systems good candidates for solar cell applications.

On the other hand, the mBJLDA scheme as carried out by Tran and collaborators [49–51] represents adequately the process structure and derivative discontinuity of the exact exchange potential. This is a significant consequence since only the semilocal terms are employed. So the semilocal orbital independent mBJLDA potential may capture the imperative of the orbital dependent potentials (hybrid functionals) and provides energy bands with reasonable exactitude in which the computed band gaps of the systems appear in gratifying accordance with the experimental evidences [9–19]. In the present work, the XC effects are considered by applying mBJLDA in order to produce with satisfactorily exactitude the electronic and optical properties of  $\text{In}_x \text{Ga}_{1-x} \text{N}$  ternary alloy (0 < x < 1).

#### 3 Results and discussions

Several physical properties of materials are straightforwardly or indirectly connected to the electronic band structure. Thus, the comprehension of the band gap of a system is valuable for its systematic utilization in optoelectronic, and electromagnetic devices. The calculations of density of states (DOS) represent the major component to investigate the electronic properties of  $In_xGa_{1-x}N$  alloys. For each concentration, the DOS was computed by using the mBJLDA approach to establish good description for the electronic structures of our considered systems. The DOS curves for various alloys are depicted in (Figs. 1a-1e). Note that the DOS for different composition of indium are almost analogous but the magnitudes of the peaks positions are not alike because of the In content variation. It is remarkably indicated that four regions occur: the first one  $(-16 \rightarrow -15 \text{ eV})$  corresponds to the

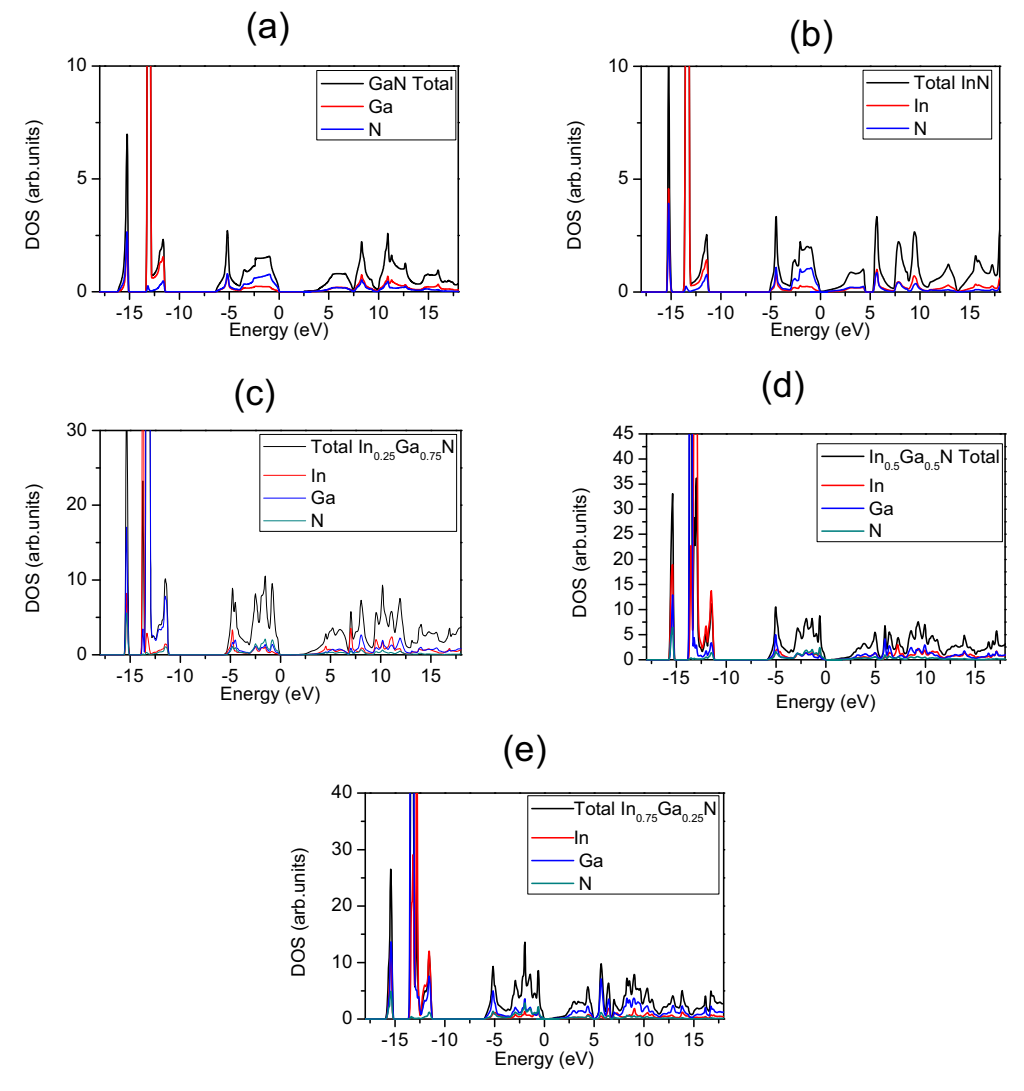


Fig. 1. Calculated total and projected density of states of GaN and InN and their alloys.

downward section of the valence bands which are strongly localized on N 2s states anion. For pure InN and GaN semiconductors, the states of the next part in the range of -13.5 and -11 eV, arise from Ga and In cations. It is apparent from the DOS of In<sub>0.25</sub>Ga<sub>0.75</sub>N, that the peaks are split in the second section of the valence states. For further In content augmentation in In<sub>0.75</sub>Ga<sub>0.25</sub>N, the splitting in the peaks is enhanced and this can be attributed to the effect of lattice mismatch between GaN and InN and d-electrons of In. For parent binary semiconductors, the splitting of these states will vanish because of the pure cation contribution. The third regime  $(-6 \rightarrow 0 \text{ eV})$  of interest in the DOS is expanded from the onset of the third to the valance band maximum at 0 eV. The DOS incorporates in this interval the uppermost of the two valance states. So, the state characters related to this region are altered mostly from cation s-like states in the band edge until the mainly p-like anion states on the band maximum. The deviation in the DOS curves is detected in the profile of the peaks that originates from the hybridization amongst the atomic orbital (the effect of Ga and In

cations), as designated in Figures 1a and 1b. It is noticeably illustrated from the curves (Figs. 1c-1e) that the influence of the cation sublattice shares the alteration of peaks locations in the uppermost section of valence states. This is due to the fact that the peak positions are different because of the variation of In content. The fourth part of the DOS involving the lowest conduction states, exhibits the assistance of p states of Ga and In atoms. Previously, it has been pointed out experimentally [1,2,5,10,33] that the crystalline growth of InGaN on sapphire substrate was handled by a plasma technique and therefore some relevant information has been identified, such as the measurement of the energy band gap, the solid composition though the X-ray diffraction, transmission spectra, and solid composition at room-temperature photoluminescence (PL), respectively. Accordingly, the resulting bowing parameter was attained around 1 eV. The relationship between the solid concentration and band gap energy has been also achieved experimentally [34,35] by considering the effects of the strain for the coherent growth of InGaN alloys on GaN. The resulting bowing parameter was about

3.2 eV, which is sufficiently greater than the previous reported values [34,35]. Moreover, the electronic and optical properties of cubic  $Ga_{1-x}In_xN$  alloys are accommodated with the modification of In content that we will present them theoretically in our study.

For the parent GaN, and InN binary compounds, we optimized the lattice parameters and those corresponding to their ternary alloys having mixed cations, are selected through Vegard's law. The lattice parameters of InGaN alloys obey the non-linear interpolation of Vegard's law. Despite the fact that the lattice mismatch between InN and GaN is nearby 13%, the aforementioned strain-induced effects may be sizeable. The alloy system follows Vegard's law and hence the lattice parameter "a" of cubic  $\text{Ga}_{1-x}\text{In}_x\text{N}$  alloy is associated to the mole fraction (x) which is expressed mathematically by the corresponding formula:

$$a_{\text{Ga}_{(1-x)}\text{In}_x\text{N}} = (1-x)a_{\text{GaN}} + xa_{\text{InN}}.$$
 (1)

The main valuable material property for designing a device is the modulation of band gap energy. With the increment of In content x from 0 to 100%, the conduction states shift as a whole, the valence states move as a whole, and therefore no new defect states occur in the band gap region. Then, the energy band gap of  $Ga_{1-x}In_xN$  alloy is determined as a function of the indium concentration x, and denoted using the following expression:

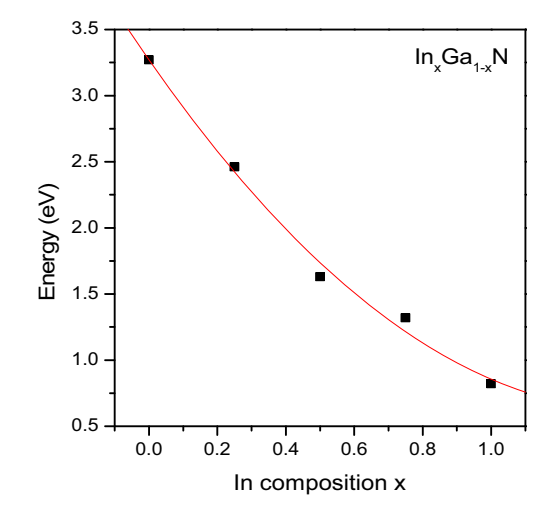
$$E_g(x) = (1-x)E_{g,GaN} + xE_{g,InN} - bx(1-x)$$
 (2)

where,  $E_g(x)$  is the energy band gap of  $Ga_{1-x}In_xN$  systems,  $E_{q,\text{InN}}$  represents the energy band gap of InN and  $E_{q,\text{GaN}}$  designates the energy band gap of GaN. b defines the band gap bowing parameter of their related  $Ga_{1-x}In_xN$  alloys and it may be dependent on the concentration. So, it is possible to investigate the relation associated to the variation of band gap values versus In concentrations from 0% to 100%. The prototype  $In_xGa_{1-x}N$ alloys exhibit direct gap behaviors, while the binary parent compounds GaN and InN are formed by a direct gap. Hereafter, from the DOS profiles of various alloys, we extracted the band gap and their respective quantities are gathered in Table 1. It is worthwhile to indicate that we utilized the mBJLDA approach to compute with sufficient accuracy the energy band gaps for both binaries and ternary compounds, as collected in Table 1. They are also compared against the other theoretical and experimental values. It is clearly noticed that our calculated values for energy gaps and lattice parameters of parent compounds are more close to the experimental data. The change of the energy gap as a function of In concentration is depicted in Figure 2. We employ a polynomial fit to the energy gap data as a function of various compositions of  $In_xGa_{1-x}N$ alloys. This relation exhibits a nonlinear behavior and it is essential to account for the second order term of Vegard's law in which the coefficient is recognized as "bowing parameter". However, no accordance was established on the magnitude of the bowing parameter, or the concern of a distinct bowing parameter characterizing the energy gap upon the whole concentration ranges [34,35,56,59].

**Table 1.** The structural parameters (units in Å) and the calculated energy band gaps  $(E_g)$  for GaN, InN compounds and their alloys (units in eV).

Alloy	Optimized lattice	Energy band
	constant (Å)	gaps (eV)
GaN	$4.48^{*}$	$3.27^{*}$
	$4^{\mathrm{a}}$	$3.30^{\rm a}$
	$4.52^{c}$	$3.21^{\rm e}$
	$4.45^{\mathrm{d}}$	$3.28^{\mathrm{f}}$
${\rm In}_{0.25} {\rm Ga}_{0.75} N$	$4.62^{*}$	$2.46^{*}$
$\rm In_{0.5}Ga_{0.5}N$	$4.73^{*}$	$1.63^{*}$
${\rm In}_{0.75} {\rm Ga}_{0.25} N$	$4.85^{*}$	$1.32^{*}$
InN	$4.96^{*}$	$0.72^{*}$
	$4.98^{c}$	$0.78^{a}$
	$4.92^{\rm b}$	$0.75^{\mathrm{e}}$

<sup>\*</sup>Present work.  $^{a}[61]$  exp.;  $^{b}[9]$  other work;  $^{c}[8]$  exp.;  $^{d}[12]$  other work;  $^{e}[26]$  other work;  $^{f}[11]$  exp.



 ${\bf Fig.~2.}$  Band gap energy as a function of In concentration.

Therefore, Figure 2 exhibits that at low In composition a prominent downward bowing can be obtained, but at immense In composition the bowing could be insignificant. Then, it is possible to characterize the alloy band gap emploving a distinct bowing parameter. It is worthwhile to indicate that at the low-In-content regime which is actually of extreme relevance for LED's and lasers, the bowing parameter could be significantly greater than the value obtained through a fit upon the thorough alloy regime. For In-rich regime (x>0.5), the system may affront some perplexities for a perfect experimental characterization [35]. As a matter of fact, the mBJLDA energy gaps fit with satisfaction the experimental data. The ternary alloy envelops one of the largest regimes in the energy gaps of overall semiconductor alloys with the variation from 0.70 eV for InN to 3.3 eV for GaN. Also, the band gap acquired through the mBJLDA is concentration dependent.

Note that the band gap energies decrease nonlinearly with increasing the x concentration and providing an average value of gap bowing which is equal 1.6 for overall

concentrations. This deviation from Vegard's law is due to the effect of the atomic short-range order that is a result of phase separation between GaN and InN. This parameter is significant for the case of the large lattice mismatch between the two compounds which is about 13%. This bowing parameter is implied by the composition disorder, since the mixing ratio of the cations and anions is the major ingredient for accommodating the extent of disorder. Previously, it has been reported experimentally that the modulation of the energy gap is up to 2.7 eV, when In fraction changes from 0 to 50% [15–21]. It is very likely to argue about the prediction of the optical transition energy, and the peak which is detected in a photoluminescence (PL) measurement [9–13], may arise through the low In content with smallest band gap. Although the considered alloys may possess an insignificant probability to appear, it should provide a very low intensity in the PL spectrum. Therefore, the change of alloys with various contents is imperative to achieve a better prediction of the PL peak. In fact, we infer that  $In_xGa_{1-x}N$  alloys, can be plausible candidates to design theoretically tandem photovoltaic (PV) devices, where the optimum band gaps absorbing photon energy varies between 0.8 eV of infrared and 3.27 eV of ultraviolet regimes. So in our work, it has been indicated that for In poor region (x less or equal 25%) the In<sub>0.25</sub>Ga<sub>0.75</sub>N may offer the possibility of pertinent band gap engineering for solar cell applications. Within the variation of band gap (from 0.7 eV for InN to 3.3 eV for GaN) for the cubic ternary alloy InGaN, much attention have been intensified on the admixture between these two compounds to constitute the alloys of the choice that are active layer in the LEDs and LDs. In fact, this system could operate all over the blue and green visible regimes.

The interaction of electromagnetic radiations with a material is characterized through the optical properties and a main factor namely, the dielectric function plays a key role for exploring the optical properties of a compound. A material's absorption spectrum represents the fraction of incident radiation which can be absorbed through a material over a regime of frequencies. The absorption spectrum is principally resolved through the optical transition between different states of a material. The dielectric function has a complex behavior and  $\varepsilon(\omega) = \varepsilon_1(\omega) + i\varepsilon_2(\omega)$  describes the material response to the photon spectrum. Other optical properties can be derived through the dielectric function. The imaginary part of the dielectric function  $\varepsilon_2(\omega)$  denotes the optical absorption in the crystal, which can be obtained from the momentum matrix elements between the filled and the vacant wave functions. It designates the change of interband transitions in a semiconductor, and the real part  $\varepsilon_1(\omega)$  is estimated through the imaginary part  $\varepsilon_2(\omega)$  by employing the Kramer-Kronig transformation.

$$\varepsilon_1(\omega) = 1 + \frac{2}{\pi} P \int_0^\infty \frac{\dot{\omega} \varepsilon_2(\dot{\omega})}{\dot{\omega}^2 - \omega^2} d\dot{\omega}. \tag{3}$$

The static dielectric constant  $\varepsilon_1(0)$  without any participation coming through the lattice vibration is inversely

proportional property which may be discerned in the framework of Penn model formulation

$$\varepsilon_1(0) \approx 1 + (\hbar \omega_p / E_g)^2$$
. (4)

The imaginary part of  $\varepsilon(\omega)$  is computed according to the well-recognized expression:

$$\operatorname{Im}\left[\varepsilon^{jj}(\omega)\right] = \frac{e^{2}\hbar^{2}}{\pi m^{2}\omega^{2}} \sum_{v,c} \left|\left\langle \psi_{c} \mid \hat{e_{j}}.P \mid \psi_{v} \right\rangle\right|^{2} \times \delta\left(E_{c} - E_{v} - \hbar\omega\right)$$
(5)

where  $\hat{e_j}$  represents the unitary vector onward the direction of the external electromagnetic field of energy  $\hbar\omega$ .  $\psi_v$  and  $\psi_c$  designate the vacant and occupied level eigenfunctions of the system, respectively and  $E_v$  and  $E_c$  represent their accompanied energies. e and m are the charge and mass of the bare electron and p denotes the momentum operator. Utilizing the spectra of real and imaginary parts of dielectric functions, it is feasible to compute the spectra of remaining optical components like, the refractive index, reflectivity, absorption coefficient and so forth.

It is worth mentioning to indicate equation (5) does not incorporate the excitonic effects. The major optical characteristics deduced from the traditional DFT calculations can be maintained approximately. By envisaging the excitonic effects, an analogous result is also achieved [62]. The local-field effects, i.e. the variation of the cell periodic term of the potential, are also ignored in equation (5). It is well recognized from the dielectric-spectra calculations, the dielectric constants may be decreased even though the local-field effects are taken into account [63]. It has been evaluated previously that the local-field effects diminish the dielectric constant of GaN around 9% [64]. The electronic self-energy corrections can enhance the band gap and decrease the dielectric constant of the system. For GaN, the dielectric constant diminishes almost around 15% because of the reduction of the band gap, whilst the electronic self-energy corrections are supplemented [65]. Hence, the  $\varepsilon_2$  spectra may be more ameliorated whenever the previous three prominent effects are incorporated. The selection of acceptable dielectric spectra can be deduced approximately from the mBJLDA scheme. Hence we chose equation (5) to compute the dielectric spectra of GaN, InN and  $In_xGa_{1-x}N$  alloys at low computation price. The current calculations on GaN also exhibit that the common behaviors of the optical spectra corroborate somehow the previous experiments and theoretical calculations.

We present here the significant impact of the composition x of In on the optical properties of the cubic ternary alloys InGaN. The dielectric functions of  $\text{In}_x\text{Ga}_{1-x}\text{N}$  alloys with various In compositions are analyzed in detail. For the binary GaN and InN and their alloys, the imaginary dielectric function is indicated in Figures 3a–3e.  $\varepsilon_2(\omega)$  is zero until the absorption begins since the photon energy achieves the band gap energy. The commencing point of absorption and major peaks possess a blueshift in consensus with the band gap extension with the diminution of x. This feature is owing to a low band gap

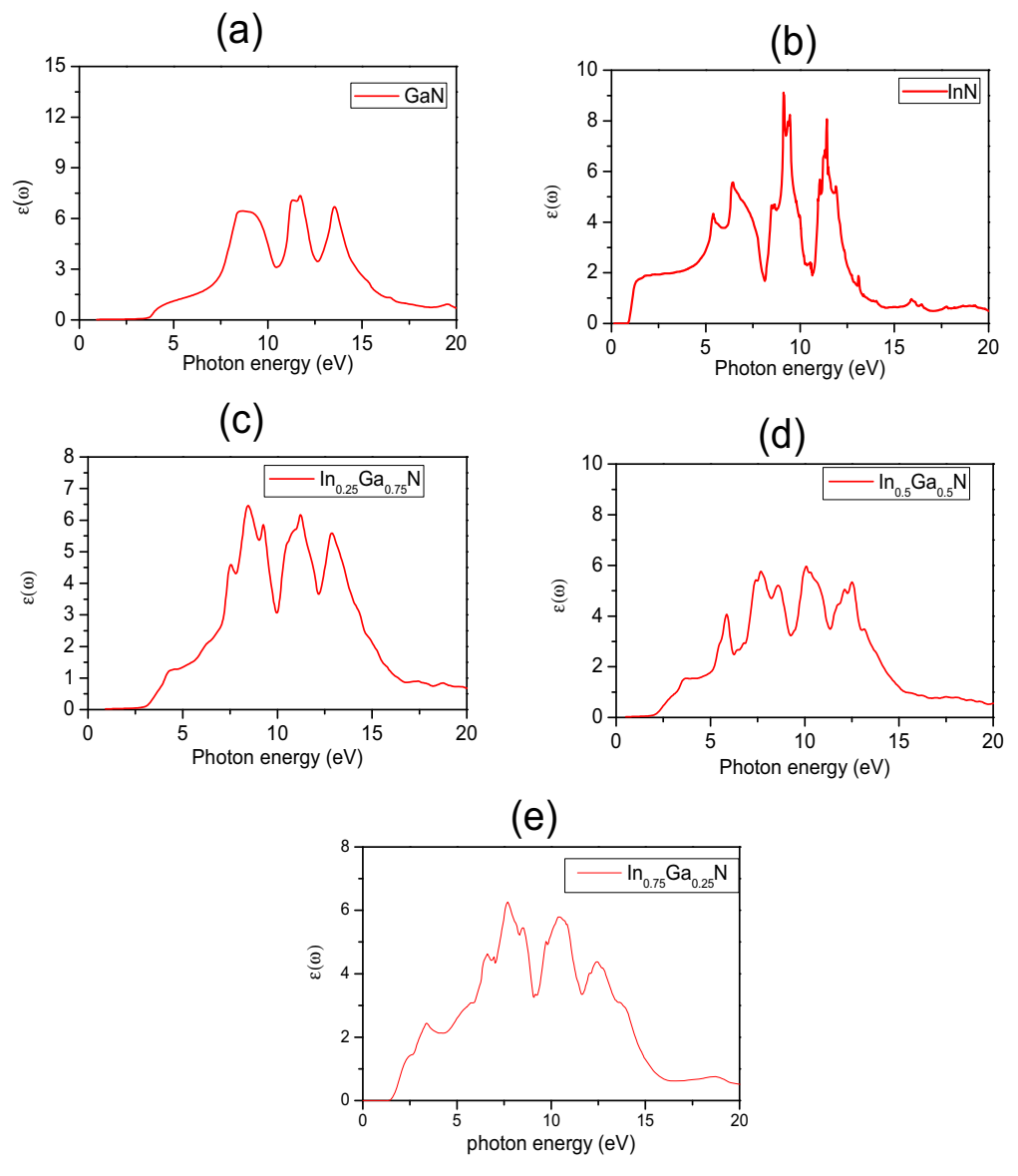


Fig. 3. Imaginary part of dielectric function of GaN, InN and their alloys.

value of InN and its participation in InGaN alloy is weakened by diminishing x. In fact, this provides an obvious indication for the enlargement of band gap alloy value and enhancement of the absorption at uppermost value of photon energy. The examination of  $\varepsilon_2(\omega)$  spectra exhibits the threshold energy arising at 3.5, 2.7, 1.85, 1.6 and 0.95 eV for GaN, In<sub>0.25</sub>Ga<sub>0.75</sub>N, In<sub>0.5</sub>Ga<sub>0.5</sub>N, In<sub>0.75</sub>Ga<sub>0.25</sub>N and InN, respectively, which are related to the direct optical transition between the resulting highest valence bands and lowest conduction bands. In common all spectra illustrate separated peaks which are accompanied to various transitions between different electronic states. It is evidently noticed from Figure 3 that  $\varepsilon_2(\omega)$  has three principal energy spectral peaks situated at 7.5, 11 and 13 eV for GaN and four major peaks occur at 5.5, 7, 9.5 and 11.5 eV for InN. For x = 0.75, the imaginary part of dielectric function is mostly prevailed by the indium peaks for first and fourth peaks around 3.5 and 11.5 eV respectively, while the Ga

content has a main participation among the second peak. For x = 0.5, we detect firstly by the occurrence of the first, and third peak by about 5.9 and 9.8 eV for InN, secondly, the second peak at 7.6 eV exhibits a mixing between GaN and InN constitutes. Finally, for x = 0.25, the peaks around 8.1, 11.8 and 13 eV are generally subjugated by GaN. For the delineation of spectra plots, it is obvious that the absorption in low energy is broadened with respect to indium reduction. One prominent feature of this optical spectrum is that the response along five different In contents is almost the same, and it changes just in the peak position and intensity. This is essentially associated to the In/Ga component ratios. For GaN case, the overall shape of  $\varepsilon_2(\omega)$  obtained from mBJLDA potential is reasonably accurate. It has been stated previously that by taking into account electron-hole interaction [64], the  $\varepsilon_2(\omega)$  spectra provide better description for the excitonic peak that is detected experimentally around 7 eV. Note that  $\varepsilon_2(\omega)$ 

is constituted principally of transition between third and fourth bands (mixture between Ga 4p and N 2p states) to fifth band (mixture between Ga 4s and N 2s states). It is worth mentioning that the difference between interacting and non-interacting energy is due to the shift of the weight to higher non-interacting energy [64]. It has been found previously that the results of electron-hole interaction can display a significant peak around 7 eV [64] which corroborates the experimental data [66]. It is evident that the electron-hole interaction shifts the peak positions as well as the peak heights, and this situation is in sharp contrast with our results. In our mBJLDA results, the peak positions are shifted to higher energies with respect to those obtained from interacting system and experiment. Also, the peak heights are reduced with the increase of energy in both non-interacting and interacting results [64]. However, the reduction of peak heights is more significant in the interacting case. In general, the mBJLDA results for  $\varepsilon_2(\omega)$  are quite striking with respect to those obtained experimentally [66] and theoretically [64]. It is evident that the limitations of mBJLDA results is due to the omission of electron-hole interaction in  $\varepsilon_2(\omega)$ , since it is based on non-interacting energy calculations.

It is worthwhile to recognize that the transparent material possesses an insignificant absorption coefficient than that of opaque one. The measurement of the absorption of light is one of the most prominent techniques for identifying the optical behavior in materials. The absorption coefficient,  $\alpha$ , is a property to characterize a material which designates the amount of light absorbed through it. Accordingly, note that the inverse of the absorption coefficient  $\alpha^{-1}$  represents the average path to be traveling over a photon before its absorption. For photon energy less than the energy gap, the creation of electron hole pairs will not appear. Then, the material is transparent and  $\alpha$ is insignificant. For photon energy more than the energy gap, the absorption is substantial. Note that the threshold frequency diminishes as In concentration is enhanced, this is not astonishing since the energy gap is reduced as In contents augment. Optical absorption is extended with the increment of photon energy. The absorption coefficient is computed from the imaginary part of the dielectric function [67]:

$$\alpha(\omega) = \sqrt{2}\omega \left[ \left\{ \varepsilon_1^2(\omega) + \varepsilon_2^2(\omega) \right\}^{1/2} - \varepsilon_1(\omega) \right]^{1/2}.$$
 (6)

Furthermore, the computed absorption coefficient can be expressed by Beer's relation [67]

$$\alpha = \frac{2k\omega}{c} = \frac{4\pi k}{c},\tag{7}$$

k is the extinction coefficient. The optical absorption coefficient is the principal feature of our considered systems. For InGaN alloys, this quantity illustrates a sharp onset (3.5, 2.5, 1.8, 1.4 and 0.9 eV for GaN, In<sub>0.25</sub>Ga<sub>0.75</sub>N, In<sub>0.5</sub>Ga<sub>0.5</sub>N, In<sub>0.75</sub>Ga<sub>0.25</sub>N and InN, respectively) followed nearly by a plateau. This deviation from the square-root dependence is anticipated to be elucidated by the appearance of a strong nonparabolic behavior of the contributing

states. This feature is evident in the representation denoted in Figures 4a–4e. From the optical absorption coefficient curves, a band gap originates downward 1 eV for InN and upward 3 eV for GaN and hence for InGaN alloys, the band gap is involved in this span (1–3 eV). According the behavior of the absorption coefficient, it is lucidly to designate the existence of two primary sections in GaN, InN and their resulting alloys. The first region exhibits the low absorption for the associated energy values in the interval  $3.5 \to 7, 2.5 \to 6.5, 1.8 \to 3.75, 1.4 \to 5 \text{ and } 0.9 \to 4.7$ for GaN,  $\rm In_{0.25}Ga_{0.75}N,\ In_{0.5}Ga_{0.5}N,\ In_{0.75}Ga_{0.25}N$  and InN, respectively. The second region illustrates the prominent absorption for particular energy values in the range  $7 \to 8.6, 6.5 \to 7.7, 3.75 \to 5.5, 5 \to 7.4 \text{ and } 4.7 \to 7 \text{ for }$ GaN,  $In_{0.25}Ga_{0.75}N$ ,  $In_{0.5}Ga_{0.5}N$ ,  $In_{0.75}Ga_{0.25}N$  and InN, respectively. The onset energies are accompanied with the energy gap change with In content ratio. For the considered alloys, the absorption is significant in the energy range between 1.1 and 7 eV, which is associated to wavelength from 1.05 to 0.17  $\mu$ m. This envelops the entire visible spectrum. From the absorption coefficient data of various energies, we can obtain the information about the band gaps of our systems. The knowledge of these band gaps is extremely substantial for comprehending the electronic properties of our systems. It is however of practical relevance for optoelectronic properties of these promising materials.

The energy gap and refractive index of semiconducting materials represent two essential physical perspectives which provide their electronic and optical characteristics. The fundamental correlation between these two factors employs the common concept of photoconductivity for semiconductors. Accordingly, their applications for optoelectronic devices are mostly ruled through the magnitude and character of these two basic semiconducting material properties. They also assist in the fulfillment evaluation for the band engineered structures for steady and optimal absorption of immense band spectral origins. Consequently, the energy gap is the major factor to resolve the threshold for absorption of photons in the material semiconductors. The refractive index provides the measurement of transparency to incident spectral relationship inside the semiconductors. It has been proposed recently in reference [68] an appealing universal fruitful relation among refractive index and energy gap, while it is viable to compute the refractive index of broad series of insulators, semiconductors, halides, and oxides. In this model, the refractive index is related to the plasmon energy and it has been proposed as an important relationship between the refractive index, energy gap and optical electro-negativity. It has been successfully applied to various semiconductors. However the relation of refractive index is the modified model of original Moss relation [68] with a second arbitrary constant (0.365) added to ameliorate the results. This provides better compromise with the experimental determinations than Moss form [69].

The models pointed out by earlier researchers have been successfully employed for the determination of the refractive index for systems with moderate adequacy,

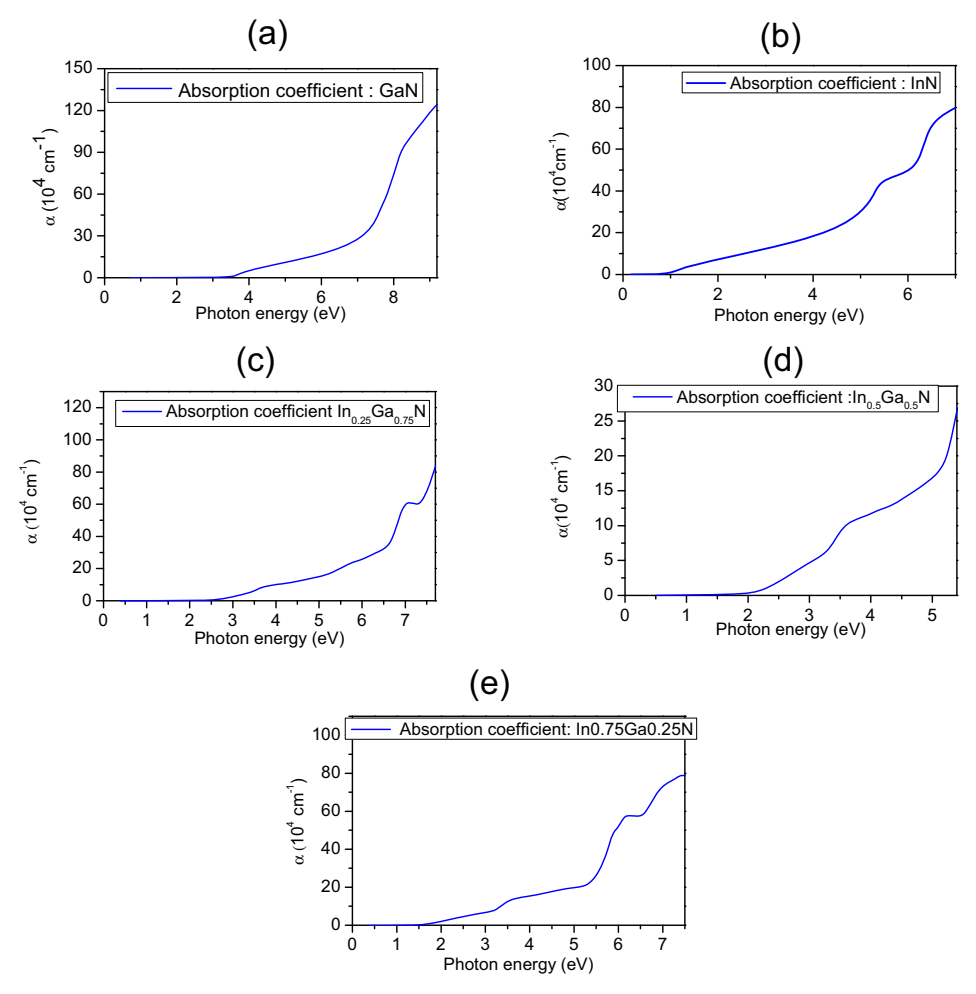


Fig. 4. Absorption coefficient of GaN, InN and their alloys.

although for restricted number of materials. Some models are suitable for narrow energy gap and some for wide energy gap materials however none of them is exactly employed for the entire regime of energy gap of semiconducting materials. Here, we compute the refractive index for various concentrations of indium by using the model proposed in reference [68] which gives reasonable values of refractive indices of various systems, as indicated in Table 2. Using the relation below, the variation of the refractive index is calculated as a function of the composition of indium.

$$n = \sqrt{\frac{12.417}{E_g - 0.365}}. (8)$$

Figure 5 exhibits the relation between the calculated refractive index versus the In contents. It is apparent that the refractive index is enhanced with the increment of composition x. The refractive index is dependent nonlinearly on the concentration. Hence, a bowing parameter owing to the lattice mismatch between the two constituent binary alloys is around 2.6. The refractive index of  $\text{In}_x \text{Ga}_{1-x} \text{N}$  obeys to the similar relation which governs the band gap assessments,

$$n_{\text{In}_x\text{Ga}_{1-x}\text{N}}(x) = (1-x)n_{\text{GaN}} + xn_{\text{InN}} - bx(1-x).$$
 (9)

 ${\bf Table~2.}$  The calculated refractive index of GaN and InN and their alloys.

Material	n
GaN	$2.07^*$ $2.28^a$ $2.3^b$ $2.31^c$ $2.34^d$
$\mathrm{In}_{0.25}\mathrm{Ga}_{0.75}\mathrm{N}$	$2.43^{*}$
$\rm In_{0.5}Ga_{0.5}N$	$3.13^{*}$
$\mathrm{In}_{0.75}\mathrm{Ga}_{0.25}\mathrm{N}$	$3.61^{*}$
InN	$5.22^{*}$

<sup>\*</sup>Present work. <sup>a</sup>[68]; <sup>b</sup>[28]; <sup>c</sup>[69]; <sup>d</sup>[70].

## 4 Conclusion

In this work, we simulated the electronic and optical properties of bulk InN and GaN and their related ternary alloys. Our theoretical contribution is to support the experimental realizations since it has been shown previously

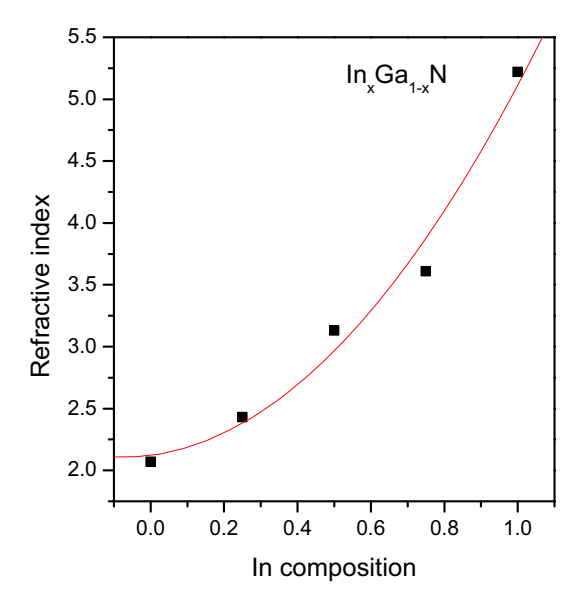


Fig. 5. Refractive index as a function of In concentration.

that the InGaN systems possess potential optical properties such as light-emitting applications. So, our goal was to modulate the energy gaps that are convenient to design theoretically InGaN-based solar cells. It has been found in the earlier experimental works that these systems are suitable for photovoltaic applications and this is based on the variation of In content (from 0% to 50%). Our results are summarized in the following essential points.

- We supplemented the electronic structure calculations for InGaN alloys, by selecting the mBJLDA approach to determine the energy band gaps within the DFT at a cheap computational price. Our results are compared with respect to the available previous theoretical findings and experimental data. The mBJLDA results are notably good for predicting the band gaps and the relevant bowing parameter fits surprisingly well the experimental realizations for the alloys investigated. This work elucidates that the mBJLDA is a propitious scheme to explore the properties of electronic states of extensive and complicated semiconducting compounds with a very low computational cost.
- The calculated energy gap of bulk InGaN alloys decreases non-linearly as In concentration increases. We asset a quite significant bowing through various In content, denoting that a concentration-independent bowing parameter characterizes the band gap of InGaN alloys. The calculated density of state is affected by In orbital contribution in the bulk InGaN alloys. This is accompanied with the enhancement in the valence bands width because of the (hybridization) admixture between the In p and d states toward the highest valence states. It is also found that the calculated refractive index of bulk InGaN alloys demonstrates its non-linear dependence on the compositions and its value increases with increasing In concentration
- The calculated absorption coefficient of bulk InGaN alloys surmises that the absorption is significant in

the energy range from 1.18 to 7 eV. This corresponds to the wavelength variation from 1.05 to 0.17  $\mu$ m. The calculated imaginary part of dielectric function of bulk InGaN alloys indicates that the starting point of absorption and main peaks have a blue-shift in accordance with decreasing In concentration. For these alloys, all energy gaps incorporate a whole range of energies (0.7–3.2 eV) which are appropriate to design theoretically solar cells with high efficiency.

The authors would like to extend their sincere appreciation to the Deanship of Scientific Research at King Saud University for its funding of this research through the Research Group Project no.: RGP- VPP-233.

## References

- 1. F.A. Ponce, D.P. Bour, Nature 386, 351 (1997)
- 2. S. Nakamura, Science 281, 956 (1998)
- R. Kimura, A. Shigemori, J. Shike, K. Ishida, K. Takahashi, J. Cryst. Growth 251, 455 (2003)
- S.V. Novikov, N.M. Stanton, R.P. Campion, R.D. Morris, H.L. Geen, C.T. Foxon, A.J. Kent, Semicond. Sci. Technol. 23, 015018 (2008)
- J. Suda, T. Kurobe, S. Nakamura, H. Matsunami, Jpn J. Appl. Phys. 39, L1081 (2000)
- S.J. Perton, C.R. Abernathy, M.E. Overberg, G.T. Thaler,
   D.P. Norton, N. Theodoropoulou, A.F. Hebard, Y.D. Park,
   F. Ren, J. Kim, L.A. Boatner, J. Appl. Phys. 93, 1 (2003)
- E. Silveira, J.E. Freitas, B. Schujman, L.J. Schpwalter, J. Cryst. Growth 310, 4007 (2008)
- 8. A. Trampert, O. Brandt, K.H. Ploog, in *Crystal structure of group III Nitrides*, edited by J.I. Pankove, T.D. Moustakas, Semiconductors and Semimetals (Academic, San Diego, 1998), Vol. 50
- K. Kim, W.R.L. Lambrecht, B. Segall, Phys. Rev. B 53, 16310 (1996)
- 10. S. Nakamura, Solid State Commun. 102, 237 (1997)
- V. Bougrov, M.E. Levinshtein, S.L. Rumyantsev, A. Zubrilov, in *Properties of Advanced Semiconductor Materials GaN, AlN, InN, BN, SiC, SiGe* edited by M.E. Levinshtein, S.L. Rumyantsev, M.S. Shur, (John Wiley & Sons Inc., New York, 2001), pp. 1–30
- S. Logothetidis, J. Petalas, M. Cardona, T.D. Moustakas, Phys. Rev. B 50, 18017 (1994)
- R. Singh, D. Doppalapudi, T.D. Moustakas, Appl. Phys. Lett. 70, 9 (1997)
- B.N. Pantha, J. Li, J.Y. Lin, H.X. Jiang, Appl. Phys. Lett. 93, 182107 (2008)
- A. Tabata, L.K. Teles, L.M.R. Scolfaro, J.R. Leite, A. Kharchenko, T. Frey, D.J. As, D. Schikora, K. Lischka, J. Furthmuller, F. Bechstedt, Appl. Phys. Lett. 80, 769 (2002)
- S. Pereira, M.R. Correia, E. Alves, Adv. Mater. Forum III, 514, 38 (2006)
- S. Pereira, M.R. Correia, E. Pereira, K.P. O'Donnell, C. Trager\_Cowan, F. Sweeney, E. Alves, Phys. Rev. B 64, 205311 (2001)
- O. Jani, I. Ferguson, C. Honsberg, S. Kurtz, Appl. Phys. Lett. 9, 132117 (2007)
- C.J. Neufeld, N.G. Toledo, S.C. Cruz, M. Iza, S.P. DenBaars, U.K. Mishra, Appl. Phys. Lett. 93, 143502 (2008)

- R. Dahal, B. Pantha, J. Li, J.Y. Lin, H.X. Jiang, Appl. Phys. Lett. 94, 63505 (2009)
- 21. S. Adachi, Properties of Group-IV, III-V, and II-VI Semiconductors (Wiley, New York, 2005)
- 22. M.D. McCluskey, C.G. Van de Walle, L.T. Romano, B.S. Krusor, N.M. Johnson, J. Appl. Phys. **93**, 4340 (2003)
- 23. S.H. Park, S.L. Chuang, J. Appl. Phys. 87, 353 (2000)
- C.J. Neufeld, N.G. Toledo, S.C. Cruz, M. Iza, S.P. DenBaars, U.K. Mishra, Appl. Phys. Lett. 93, 143502 (2008)
- T. Kuykendall, P. Ulrich, S. Aloni, P. Yang, Nat. Mater. 6, 951 (2007)
- S.Q. Wang, H.Q. Ye, J. Phys.: Condens. Matter 14, 9579 (2002)
- J.S. Thakur, A. Dixit, Y.V. Danylyuk, C. Sudakar, V.M. Naik, W.J. Schaff, R. Naik, Appl. Phys. Lett. **96**, 181904 (2010)
- 28. H. Harima, J. Phys.: Condens. Matter 14, R967 (2002)
- P.D.C. King, T.D. Veal, C.E. Kendrick, L.R. Bailey, S.M. Durbin, C.F. McConville, Phys. Rev. B 78, 033308 (2008)
- K. Shimomoto, A. Kobayashi, K. Ueno, J. Ohta, M. Oshima, H. Fujioka, H. Amanai, S. Nagao, H. Horie, Phys. Status Solidi (RRL) 3, 124 (2009)
- R. Dahal, B. Pantha, J. Li, J.Y. Lin, H.X. Jiang, Appl. Phys. Lett. 94, 063505 (2009)
- T. Kuykendall, P. Ulrich, S. Aloni, P. Yang, Nat. Mater. 6, 951 (2007)
- Po Shan Hsu, Kathryn M. Kelchner, Anurag Tyagi, Robert M. Farrell, Daniel A. Haeger, Kenji Fujito, Hiroaki Ohta, S.P. Den Baars, J.S. Speck, Shuji Nakamura, Appl. Phys. Express 3, 052702 (2010)
- M. van Schilfgaarde, A. Sher, A.-B. Chen, J. Cryst. Growth 178, 8 (1997)
- 35. A. Baldanzi, E. Bellotti, M. Goano, Phys. Stat. Sol. B **228**, 425 (2001)
- 36. P. Holenberg, W. Kohn, Phys. Rev. B 136, 864 (1964)
- 37. W. Kohn, L.S. Sham, Phys. Rev. **140**, A1133 (1965)
- 38. J.P. Perdew, S. Burke, M. Ernzerhof, Phys. Rev. Lett. **78**, 1386 (1997)
- O. Gunnarsson, B.I. Lundqvist, Phys. Rev. B 13, 4274 (1976)
- 40. J.P. Perdew, Y. Wang, Phys. Rev. B 45, 13244 (1992)
- M. Gruning, A. Marini, A. Rubio, Phys. Rev. B 74, 161103(R) (2006)
- 42. S. Kummel, L. Kronik, Rev. Mod. Phys. 80, 3 (2008)
- S. Sharma, J.K. Dewhurst, C. Ambrosch-Draxl, Phys. Rev. Lett. 95, 136402 (2005)
- W.G. Aulbur, M. Städele, A. Görling, Phys. Rev. B 62, 7121 (2000)

- R.J. Magyar, A. Fleszar, E.K.U. Gross, Phys. Rev. B 69, 045111 (2004)
- 46. L. Hedin, Phys. Rev. A **139**, 796 (1965)
- 47. M.S. Hybertsen, S.G. Louie, Phys. Rev. Lett. **55**, 1418 (1985)
- V.I. Anisimov, J. Zaanen, O.K. Andersen, Phys. Rev. B 44, 943 (1991)
- F. Tran, P. Blaha, K. Schwarz, J. Phys.: Condens. Matter 19, 196208 (2007)
- 50. F. Tran, P. Blaha, Phys. Rev. Lett. 102, 226401 (2009)
- 51. P. Haas, F. Tran, P. Blaha, Phys. Rev. B 79, 085104 (2009)
- 52. D.J. Singh, Phys. Rev. B 82, 205102 (2010)
- 53. D. Koller et al., Phys. Rev. B 83, 195134 (2011)
- San-Dong Guo, Bang-Gui Liu, Europhys. Lett. 93, 47006 (2011)
- 55. Wanxiang Feng et al., Phys. Rev. B 82, 235121 (2010)
- R.R. Pelá, C. Caetano, M. Marques, L.G. Ferreira, J. Furthmüller, L.K. Teles, Appl. Phys. Lett 98, 151907 (2011)
- J. Heyd, G.E. Scuseria, M. Ernzerhof, J. Chem. Phys. 118, 8207 (2003)
- J. Heyd, G.E. Scuseria, M. Ernzerhof, J. Chem. Phys. 124, 219906 (2006)
- P.G. Moses, C.G. Van de Walle, Appl. Phys. Lett. 96, 021908 (2010)
- 60. P. Blaha, K. Schwarz, G.K.H. Madsen, D. Kvasnicka, J. Luitz, WIEN2K: An Augmented Plane Wave plus Local Orbitals Program for Calculating Crystal Properties (Vienna University of Technology, Austria, 2001)
- T. Lei, T.D. Moustakas, R.J. Graham, Y. He, S.J. Berkowitz, J. Appl. Phys. 71, 4933 (1992)
- P. Rinke, M. Scheffler, A. Qteish, M. Winkelnkemper, D. Bimberg, J. Neugebauer, Appl. Phys. Lett. 89, 161919 (2006)
- R. Laskowski, N.E. Christensen, G. Santi, C. Ambrosch-Draxl, Phys. Rev. B 72, 035204 (2005)
- 64. L.X. Benedict, E.L. Shirley, Phys. Rev. B 59, 5441 (1999)
- 65. M. Palummo, L. Reining, R.W. Godby, C.M. Bertoni, N. Bornsen, Europhys. Lett. **26**, 607 (1994)
- C. Janowitz, M. Cardona, R.L. Johnson, T. Cheng, T. Foxon, O. Gunther, G. Jungk, BESSY Jahresbericht Report No. 230 1994 (unpublished)
- M. Fox, Optical Properties of Solids (Oxford University Press, 2001)
- 68. R.R. Reddy et al., Opt. Matter 31, 209 (2008)
- 69. T.S. Moss, Phys. Stat. Sol. B 131, 415 (1985)
- U. Köhler, D.J. As, B. Schöttker, T. Frey, K. Lischka, J. Scheiner, S. Shokhovets, R. Goldhahn, J. Appl. Phys. 85, 404 (1999)